Enhancement of Two-Photon Absorption Cross-Section in Macrocyclic Thiophenes with Cavities in the Nanometer Regime

Ajit Bhaskar,[†] Guda Ramakrishna,[†] Kevin Hagedorn,[†] Oleg Varnavski,[†] Elena Mena-Osteritz,[‡] Peter Bäuerle,[‡] and Theodore Goodson III*,[†]

Department of Chemistry and Department of Macromolecular Science and Engineering, University of Michigan, Ann Arbor, Michigan 48109, and Department of Organic Chemistry II, Ulm University, 89081 Ulm, Germany

Received: October 14, 2006; In Final Form: November 29, 2006

The linear and nonlinear optical properties of two thiophene-based cyclic molecules have been investigated. These molecules represent nanometer sized cavities which may be useful for novel photonic devices. By virtue of long-range interactions, these chromophores serve as novel architectures for enhanced two-photon absorption (TPA) properties. Measurements of the different size ring structures showed a 550% increase in the TPA cross-section for the larger macrocycle. Electronic structure calculations have suggested an increase in coupling of the excited states in these systems as the ring size is increased. Measurements of the ultrafast transient absorption and fluorescence were carried out with these systems in order to probe the interaction between the chromophores. The results of the transient decays as well as fluorescence anisotropy decay times gives stronger proof to the suggestion of delocalized states in the cyclic macrocycles. These results provide information regarding the optical properties of these novel systems useful for potential applications in photonics.

1. Introduction

The search for new optical devices has inspired the creation of novel materials with tailored structure−property relationships. Multi-chromophore and self-assembly approaches have been applied toward the creation of superior light harvesting, light emitting, and nonlinear optical materials. This has included organic polymers, dendrimers, rotaxanes, fullerenes, and two-dimensional bis-annulene structures.[1−3] An important characteristic that is common to many of these materials is that the multi-chromophore architecture possesses collective excitations where several chromophores in the architecture contribute to the optical response. For applications involving nonlinear optical (NLO) processes, this collective behavior is utilized and it results, in some cases, in enhancing properties beyond what is expected for the isolated or localized set of chromophores. Previous reports with regard to organic branched structures have categorized the excitations in such systems as either incoherent (a hopping regime) or coherent (and strongly coupled) .[4,5] It was found that, for cases of coherent interactions in multi-chromophore systems, strong enhancement of the two-photon absorption (TPA) effects was possible.[6] The investigation of this effect in several dendrimer systems has inspired possible applications in two-photon imaging and photodynamic therapy.

There have been reports which have related the structure−property relationships in certain organic materials such as conjugation length,[7,8] substituents,[9,10] dimensionality (dipoles, quadrupoles, and octupoles),[11−14] and intramolecular interactions[6] among others. The majority of the reports have concentrated on linear and branched architectures. In terms of particular structures, various organic chromophores have been studied for their NLO behavior as well as in photonics. In this regard, oligo- and polythiophenes are among the primary candidates for organic electronics.[15−21] They are used as hole transport materials for organic light emitting diodes (OLEDs),[22,23] field effect transistors (FETs),[24,25] photovoltaic cells,[26,27] and light modulators.[28,29] Thiophenes are more amenable to synthetic modifications by virtue of enhanced reactivity at the α and β positions of the thiophene ring. This enables one to synthesize a variety of molecules with systematic variations in the structure.[30] Donor−acceptor substituted thiophene derivatives have been investigated for their TPA behavior.[31,32] However, these investigations involved linear, quadrupolar molecules. To best of our knowledge, the nonlinear optical properties of thiophenes in geometries other than linear chromophores have not been explored in detail. For example, macrocyclic thiophenes with relatively large cavities have not been explored for their TPA properties or their collective excitations. Electronic structure calculations of thiophene-based systems have been investigated previously.[33] Marsella[34] has proposed that they can be used as molecular muscles.[34] Also, applications in biological areas have been proposed.[35−37] Other applications in optoelectronics and photonics have also been determined.[38]

In this paper, we present the optical properties of conjugated macrocyclic oligothiophenes in a circular geometry consisting of terthiophene and diacetylene units C[3T-DA]$_n$. The structures of the cyclo(terthiophene-diacetylenes) are presented in Figure 1. The advantage circular chromophores have over linear systems is that there are no "end effects", which in particular in shorter oligomers influence the conjugation length and consequently the electronic and optical properties.[33,39,40] We have studied the NLO properties of two cyclo(terthiophene-diacetylenes) with different ring sizes, the cyclodimer C[3T-DA]$_2$ and the cyclopentamer C[3T-DA]$_5$. The macrocycles include nanometer sized cavities, which renders them attractive for several potential applications. Their TPA cross-section (δ)

* To whom correspondence should be addressed. E-mail: tgoodson@umich.edu.
† University of Michigan.
‡ Ulm University.

10.1021/jp066766o CCC: $37.00
Published on Web 01/11/2007

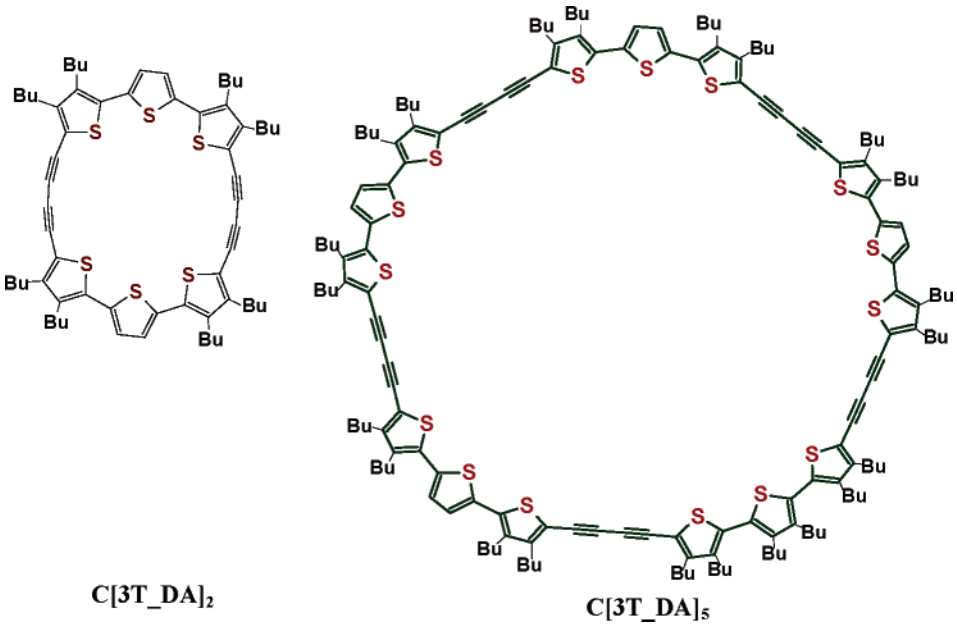

Figure 1. Structures of the macrocyclic terthiophene-diacetylenes studied in this investigation.

TABLE 1: Summary of the Linear and Nonlinear Optical Properties of Cyclothiophenes

molecule	λ_{abs} (nm)	λ_{em} (nm)	Φ^a	max (GM)	τ_{FL} (ns)
C[3T-DA]$_2$	400	540	0.04	105 (52.5)^b	0.395
C[3T-DA]$_5$	433	541	0.12	1470 (294)^b	0.408

^{a} Quantum yield was measured at 430 nm. ^{b} Figures in parentheses indicate value per [3T-DA] repeating unit.

spectra were measured using two-photon excited fluorescence (TPEF) method. We have also investigated the fluorescence dynamics and the excited-state absorption dynamics in these systems. Because the number of [3T-DA] repeating units differ in the molecule, the chromophore density in cyclopentamer C[3T-DA]$_5$ is 2.5 times higher than in the cyclodimer C[3T-DA]$_2$. An interesting question is the cooperative enhancement in TPA cross-section as a result of increase in chromophore density. The extent of enhancement might elucidate the extent of intramolecular interactions in these cyclic systems. This leads to the theoretical model of the electronic structure of these systems.

It has been found in previous theoretical studies that the main differences in the absorption spectra of cyclothiophenes in comparison to the corresponding linear oligothiophenes are caused by different selection rules as a consequence of their different geometries. The cyclothiophenes have transition dipole moments mainly arranged in the ring plane with a very small perpendicular component, which results in a forbidden S_0-S_1 transition but allowed S_0-S_2 transition. A theoretical paper on the relation between conformations of a series of cyclothiophenes (C6T-C30T) on their electronic properties, e.g., their HOMO−LUMO energy levels and gaps, has been published.[33,41] These reports showed an increase in the coupling between excited energy levels with an increase in ring size (an increase in the number of monomer chromophores).

2. Experimental Details

2.1. Synthesis and Structural Characterization. The synthesis of the two macrocycles used in this report has been previously reported.[38] Structural characterization using X-ray measurements[42] of single crystals have shown a nearly perfect circular shape for C[3T-DA]$_2$, and the diameter of the circular cavity was estimated to be 1.1 nm.

2.2. Steady-State Measurements. Unless stated otherwise, all the experiments were performed in toluene. The absorption spectra of the molecules were recorded using an Agilent (Model No. 8341) spectrophotometer. The emission spectra were acquired using a Jobin Yvon Spex Fluoromax-2 spectrofluorimeter. The quantum yields of the molecules were measured using a known procedure.[43] Coumarin 307 in methanol was used as the standard.

2.3. Two-Photon Excited Fluorescence Measurements. To measure δ, we followed the TPEF method.[44] A 10^{-4} M Coumarin 307 solution in methanol was used as the reference over a wavelength range of 700−800 nm. Fluorescein (pH = 11) was used as a standard over a 800−900 nm range. To measure the TPA cross-sections for wavelengths less than 700 nm, MSB dissolved in cyclohexane was used as the reference.[45] A mode-locked Ti:sapphire laser (Kapteyn Murnane (KM)) was used for determining δ over 760−820 nm. For the remaining wavelengths (630−760 and 820−900 nm), an optical parametric amplifier (OPA-800C, Spectraphysics) was employed. The seed used was a mode-locked Ti:sapphire laser (Tsunami, Spectra Physics). This was amplified using a regenerative amplifier (Spitfire, Spectra Physics), which in turn was pumped by a Nd:YLF laser (Empower, Spectra Physics). The amplified pulses were obtained at 1 kHz, 800 nm, and ~100 fs. This was used for pumping the OPA.

2.4. Fluorescence Lifetime Measurements. Time-correlated single-photon counting (TCSPC) was used to determine the fluorescence lifetimes of the macrocycles used in this study. The laser used was the KM system described earlier. The second harmonic from the 800 nm output was used for these measurements.

2.5. Fluorescence Up-Conversion. Time-resolved polarized fluorescence of C[3T-DA]$_5$ and C[3T-DA]$_2$ was studied using the femtosecond up-conversion spectroscopy technique. The up-conversion system used in our experiments has been previously described.[20,62] Specifically, our up-conversion system used frequency-doubled light from a mode-locked Ti:sapphire laser

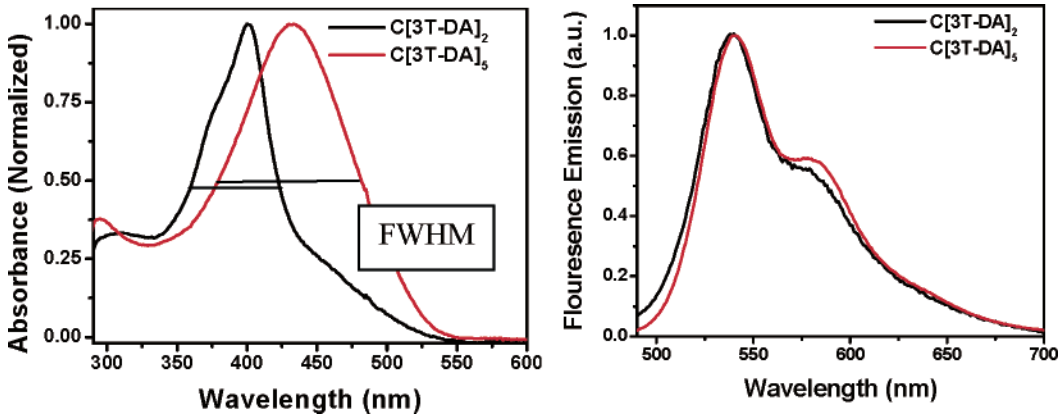

Figure 2. Absorption and emission spectra of $C[3T\text{-}DA]_2$ and $C[3T\text{-}DA]_5$.

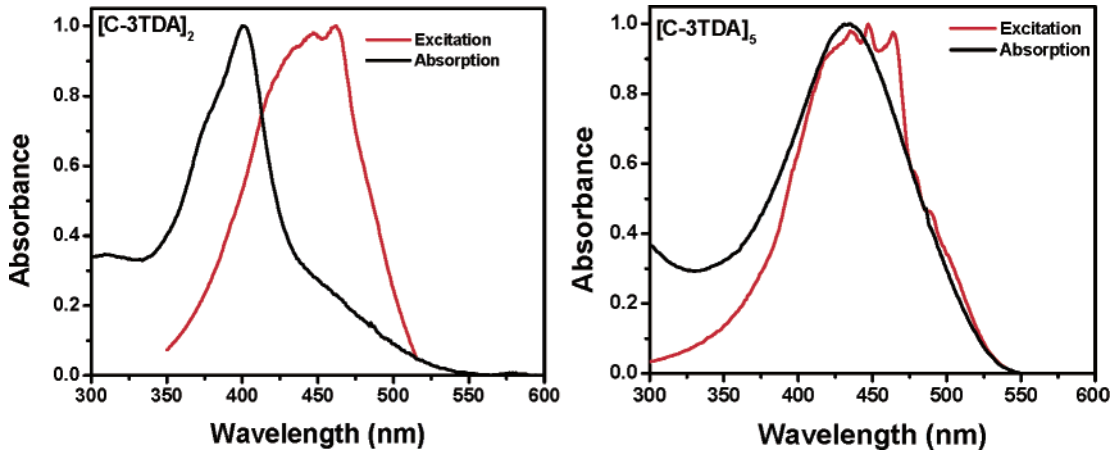

Figure 3. Excitation spectra of $C[3T\text{-}DA]_2$ and $C[3T\text{-}DA]_5$ respectively.

(385−430 nm). Polarization of the excitation beam for the anisotropy measurements was controlled using a Berek compensator, and the rotating sample cuvette was 1 mm thick. Horizontally polarized fluorescence emitted from the sample was up-converted in a nonlinear crystal of β-barium borate using a pump beam at 800 nm, which first passed through a variable delay line. Instrument response function (IRF) was measured using Raman scattering from water. Fitting the Gaussian peak from the Raman scattering yielded a σ value of ∼105 fs, which gives a full width at half-maximum of ∼240 fs. Spectral resolution was achieved by using a monochromator and photomultiplier tube. The excitation average power varied but was around 0.8 ± 0.05 mW or around 1×10^{-11} J/pulse. Under these experimental conditions, investigated thiophenes are quite stable and no photodegradation was observed.

2.6. Excited-State Measurements. Transient absorption was used to investigate the excited-state dynamics of the cyclic thiophenes. The pump beam was produced by the OPA-800C described above. The pump beams used in the present investigation were obtained from the fourth harmonic of signal and idler beams and were focused onto the sample cuvette. The probe beam was delayed with a computer-controlled motion controller and then focused into a 2 mm sapphire plate to generate a white light continuum. The white light was then overlapped with the pump beam in a 2 mm quartz cuvette containing the sample, and the change in absorbance for the signal was collected by a CCD detector (Ocean Optics). Data acquisition was controlled by the software from Ultrafast Systems Inc. Typical power of the probe beam was <0.1 μJ, while the pump beam was around ∼0.5−1 μJ/pulse. Magic angle polarization was maintained between the pump and probe using a wave plate. The pulse duration was obtained by fitting the solvent response, which was ∼130 fs. The sample was stirred with a rotating magnetic stirrer, and no photodegradation of the sample was observed.

3. Results and Discussion

The linear and nonlinear optical properties of the cyclothiophenes are summarized in Table 1. Results obtained from individual measurements are discussed below.

3.1. Optical Absorption and Steady-State Fluorescence Measurements. The absorption and emission spectra of the cyclothiophenes are presented in Figure 2. It is interesting to note that the molecules have different absorption maxima but the same emission maximum. A shoulder in the range of 440−500 nm is observed in $C[3T\text{-}DA]_2$. The absorption maximum at 400 nm is assigned to the S_0-S_2 transition according to the selection rules. The shoulder is therefore assigned to the S_0-S_1 transition. This shoulder is not seen in the absorption spectrum of $C[3T\text{-}DA]_5$. There is only one distinct absorption maximum at 433 nm. Hence, the S_0-S_2 transition shows a bathochromic shift attributed to an increase in conjugation, and it is suggested that a single peak results due to the close proximity between S_2 and S_1 states, which would now be separated by a smaller energy gap. This conclusion is further corroborated by the parameter "full width at half-maximum" (fwhm), which is 4000 cm^{-1} for the cyclodimer $C[3T\text{-}DA]_2$ and much larger for the cyclopentamer (5526 cm^{-1}).

The excitation spectra of the molecules are presented Figure 3. The absorption spectra are also provided for reference. It is seen that the excitation spectrum for $C[3T\text{-}DA]_2$ shows a bathochromic shift with respect to its absorption spectrum. This

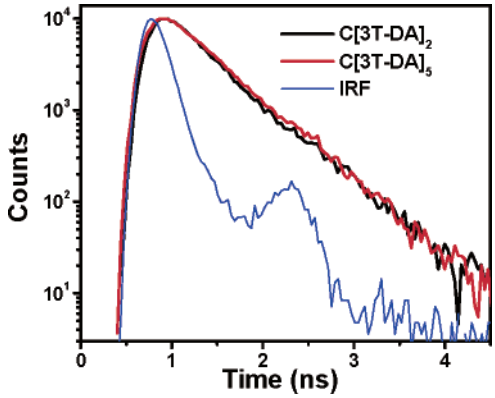

Figure 4. Normalized fluorescence decay traces for C[3T-DA]$_2$ and C[3T-DA]$_5$ obtained from TCSPC. Also shown is the IRF, the instrument response function.

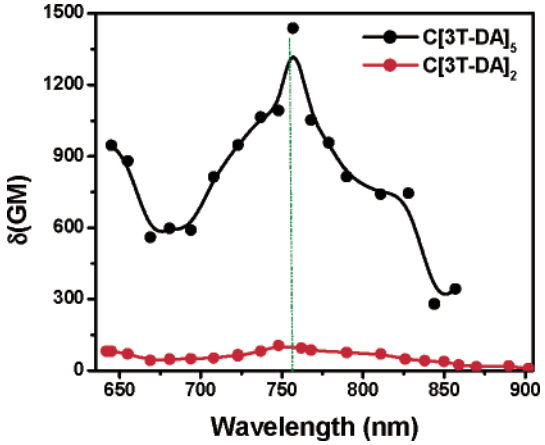

Figure 5. TPA cross-sections of C[3T-DA]$_2$ and C[3T-DA]$_5$ at different wavelengths.

indicates that the emitting state is different from the absorbing state. On the other hand, no such red shift is observed for C[3T-DA]$_5$. On the basis of these results, it is suggested that the absorbing state in both molecules is the S_2 state, whereas the emitting state is S_1. This supports the suggestion regarding the close proximity of the higher excited states in C[3T-DA]$_5$. The present excitation spectrum for C[3T-DA]$_2$, along with its absorption spectrum, also suggests that there is no emissive pathway from S_2 to ground state and that S_2 and S_1 states are not efficiently coupled.

3.2. Fluorescence Quantum Yield and Lifetime Measurements. The fluorescence quantum yields for these cyclothiophenes were measured at two excitation wavelengths, namely, 400 and 430 nm. These corresponded to S_1 and S_2 states, respectively. The fluorescence quantum yields were found to be 0.01 and 0.04 respectively for C[3T-DA]$_2$, whereas C[5T-DA]$_2$ showed a constant value of 0.12 at both excitation wavelengths. This suggests that in the case of C[3T-DA]$_2$, there is a nonradiative pathway from the S_2 state. The low quantum yields for these cyclothiophenes in general suggest that there is an efficient nonradiative decay from the S_1 state (see below). Figure 4 shows the normalized fluorescence decay traces obtained from TCSPC. The fluorescence lifetimes for C[3T-DA]$_2$ and C[3T-DA]$_5$ were found to be 395 and 408 ps, respectively. The similarity in fluorescence lifetimes again indicates that the emitting state is S1 for both molecules.

3.3. TPA Cross-Section Measurements. The TPA cross-section spectra for both rings are shown in Figure 5. It is seen that both rings show a maxima around 760 nm, suggesting that the first TPA state has a similar energetic location for both macrocycles. However, the bigger ring C[3T-DA]$_5$ shows a δ_{max} of 1470 GM which is about 14 times the δ_{max} of C[3T-DA]$_2$ (105 GM), suggesting more than an order of magnitude increase in δ. Considering that there are two [3T-DA] units, the δ per [3T-DA] unit is 52.5 GM. The same for C[3T-DA]$_5$ is 294 GM. Hence, it is seen that an increase in chromophore density by a factor of 2.5 results in 5.6 times enhancement of TPA cross-section.

The higher TPA cross-section for the larger ring suggests that the conjugation is extended over a significant fraction of the ring, if not over the entire ring. It is to be expected that these systems do not possess charge-transfer character. Considering the same, we believe that the δ values obtained for our cyclothiophene systems are quite large and even comparable with some of the quadrupolar derivatives reported in the literature.[46] Hence, we also suggest that by adding strong donor−acceptor groups to our cyclic systems, it is possible to engineer novel molecules with even higher TPA cross-sections.

3.4. Transient Absorption Measurements. As mentioned above, we are interested in the mode of energy transport and excited-state dynamics in these systems. To understand the process of excited-state deactivation of the cyclothiophenes, ultrafast transient absorption measurements have been carried out. Figure 6a shows the transient absorption at different time delays from 6 to 800 ps of C[3T-DA]$_2$ in toluene after excitation at 420 nm. At a time delay of 6 ps, excited-state absorption (ESA) with a maximum at 690 nm has been observed and has been ascribed to singlet−singlet absorption since the decay lifetime of it matched very well with the fluorescence lifetime of the molecule. As a time delay is increased from 6 to 800 ps, the singlet−singlet ESA decays with a growth in the region of 450−600 nm with a maximum at 500 nm. A clear isobestic point at 540 nm suggests that the singlet state is decayed to form a new transient which is long-lived. Figure 6b shows the kinetic decay traces at 700 and 500 nm. It can be clearly seen that there is a growth of transient at 500 nm and it is long-lived (>1 ns, time limit of instrument). Since this ESA is long-lived, it has been ascribed to triplet−triplet absorption.

Interesting transient absorption features are observed when we follow the transients at shorter time delays. Figure 7a shows the transient absorption spectra of C[3T-DA]$_2$ in toluene at time delays of 150 fs to 6 ps. Broad transient absorption from 450 to 750 nm has been observed at a time delay of 150 fs. As the time delay is increased, this broad ESA is decayed to give rise to ESA with a maximum at 690 nm with a time constant of 350 fs. This broad ESA can be attributed to S_2 state's ESA. The ESA with a maximum at 690 nm has already been ascribed to singlet-state excited-state absorption. Kinetic traces at 520 and 720 nm at a very short time scale (Figure 7b) show the initial ESA (S_2 state) decaying to give rise to the S_1 state.

Figure 7b shows the kinetic decay trace at 520 nm and the growth of transient at 720 nm. The dynamics of growth (~350 fs) and decay clearly matched, suggesting that there is an internal conversion from S_2 (Franck−Condon) to S_1 state. However, the excitation spectrum did not match with the absorption spectrum for C[3T-DA]$_2$, and it can be concluded from these results that there is an efficient nonradiative pathway (with a lifetime of ~300 fs) from the S_2 state to some other nonradiative state. If the entire population of the S_2 state were transferred to the S_1 state, we might have observed a clear isobestic point at the initial time delays, which is found to be absent suggesting that there is a cascade relaxation of population to another nonradiative

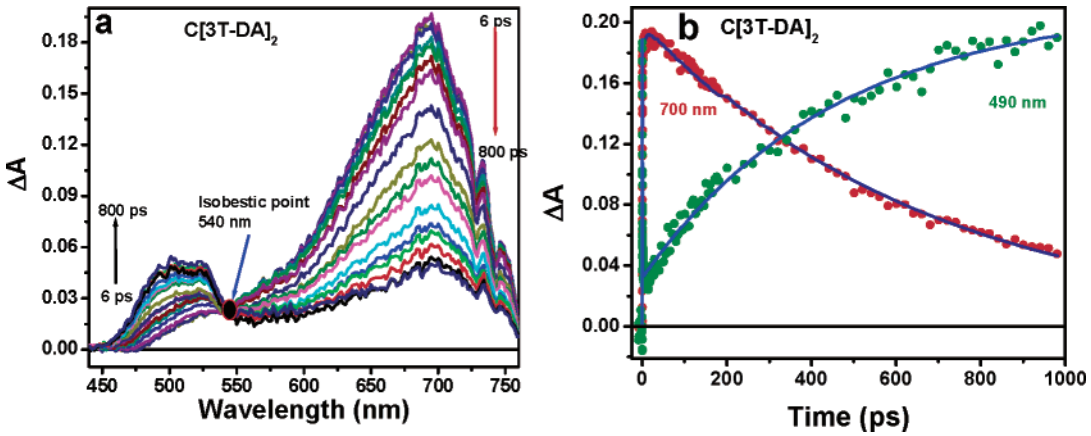

Figure 6. (a) Transient absorption of C[3T-DA]$_2$ in toluene at different time delays from 6 to 800 ps. (b) Kinetic traces at 700 and 480 nm of C[3T-DA]$_2$ in toluene after excitation at 420 nm.

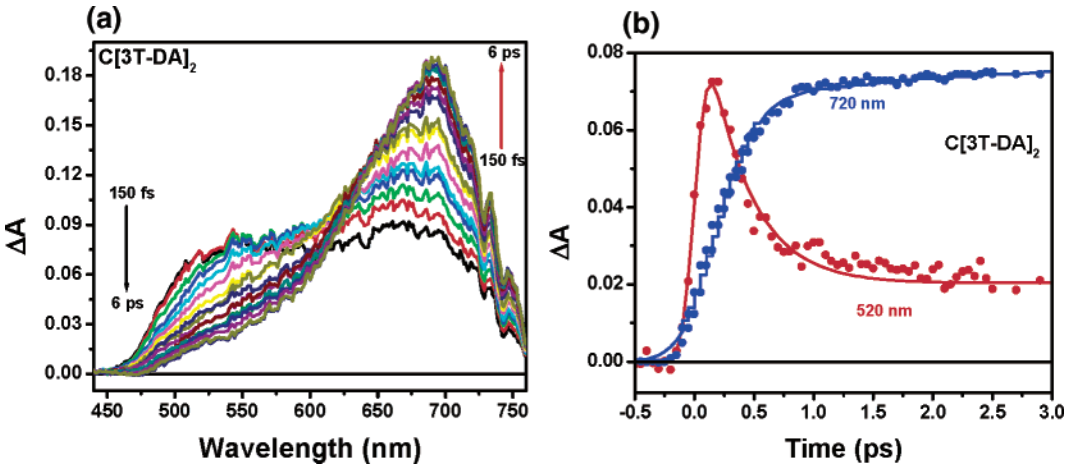

Figure 7. (a) Transient absorption of C[3T-DA]$_2$ in toluene at different time delays from 150 fs to 6 ps. (b) Kinetic traces at 720 and 480 nm of C[3T-DA]$_2$ in toluene after excitation at 420 nm.

state. However, as seen above, there is an efficient population transfer from S_1 to triplet observed (intersystem crossing, ISC; Figure 6b) with a clear isobestic point at 540 nm and with a time constant of ~350 ps. Because the ISC process is a radiationless one, it explains the low fluorescence quantum yield observed for the molecule.

It has been observed from steady-state emission measurements that C[3T-DA]$_5$ shows higher quantum yield than C[3T-DA]$_2$. In an effort to clarify the mechanism, we have carried out transient absorption measurements of C[3T-DA]$_5$ dissolved in toluene and respective excited-state absorption features, and kinetics are shown in parts a−c of Figure 8. It can be observed that observed ESA spectral features are different from C[3T-DA]$_2$. Figure 8a shows the transient absorption spectra from 6 to 800 ps. The transient absorption spectrum at a time delay of 6 ps consists of bleach in the region of 450−650 nm with characteristic bleach maxima around 490, 545, and 585 nm and a positive absorption with a maximum around 690 nm. The bleach with a maximum at 545 and 585 nm can be ascribed to stimulated emission from the S_1 state. However, the bleach with a maximum at 490 nm is due to the disappearance of ground state. As the time delay is increased, the bleach has decayed to give rise to a positive transient. The transient absorption spectrum at 800 ps had shown a positive absorption spectrum whole in the visible region from 450 to 750 nm with maxima around 520 and 690 nm. It has been observed from fluorescence measurements that the lifetime of the S_1 state of the molecule is around 400 ps, and thus the transient present at 800 ps can be attributed to triplet−triplet absorption.

It can be observed from the kinetic trace shown in Figure 8b that the stimulated emission recovers back to give rise to positive ESA corresponding to triplet-state absorption. The growth of this triplet is found to be around 300 ps, which is comparable to the observed fluorescence lifetime. However, Figure 8c shows no decay to form a triplet state. This can be because of the overlapping absorptions of singlet and triplet states. It can be observed from the kinetics shown in Figure 8b,c that there exist interesting excited-state dynamics at early time scales. Shown in Figure 9a is the transient absorption spectrum of [C-3TDA]$_5$ in a shorter time window (from 150 fs to 5 ps). Immediately after the photoexcitation at 420 nm, negative absorption with a maximum at 480 nm and positive absorptions with maxima around 540 and 700 nm are observed. The negative absorption at 480 nm is due to the bleach of ground-state absorption. The positive absorption bands at 480 and 700 nm can be ascribed to the ESA of S_2 state or to the Franck−Condon (FC) excited state of S_1. The fact that this state's ESA is decaying to S_1-state emission unambiguously suggests that both of these states are intimately connected.

The kinetic decay trace corresponding to bleach of ground-state absorption is provided in Figure 9b. The fact that there is no recovery of bleach suggests that there is no ultrafast pathway from the S_2 state back to the ground state and the S_2 state is decaying to give the stimulated emission from the S_1 state. This

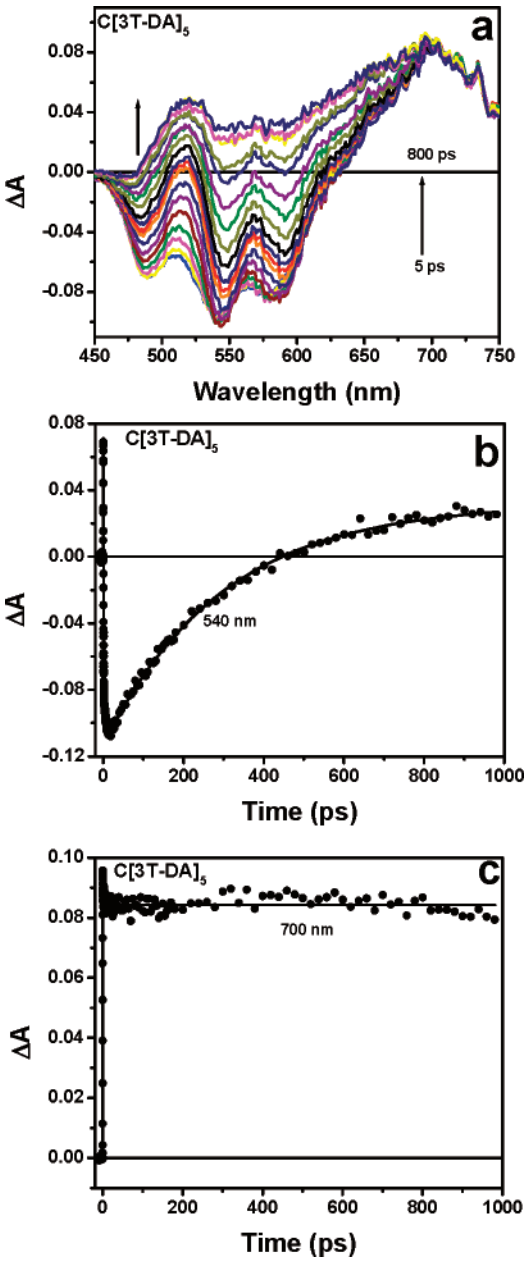

Figure 8. (a) Transient absorption spectra at different time delay from 6 to 800 ps of $[C\text{-}3TDA]_5$ in toluene after excitation at 420 nm. (b) Kinetic trace at 540 nm. (c) Kinetic decay trace at 700 nm.

information is further established by the kinetic decay trace at 520 nm shown in Figure 9c. Global fit analysis had shown that the decay time from the S_2 state to the S_1 state is around 460 fs. The presence of another nonradiative state in $C[3T\text{-}DA]_2$ observed from the transient measurements explains the lower quantum yield in $C[3T\text{-}DA]_2$ than in $C[3T\text{-}DA]_5$. The results further suggest the proximity between S_2 and S_1 states and efficient coupling between them in $C[3T\text{-}DA]_5$. Hence, these detailed transient absorption measurements confirm the existence and importance of the S_2 and S_1 states (mechanistic picture is shown in Scheme 1) in the investigated cyclothiophenes. These results also compare and elucidate the efficiency of coupling between the two states and also explain the differences in observed fluorescence quantum yields of the thiophene macrocycles.

3.6. Fluorescence Upconversion. We have also carried out fluorescence up-conversion measurements to investigate the mode of energy transport in the thiophene macrocycles $C[3T\text{-}DA]_5$ and $C[3T\text{-}DA]_2$. This technique has been extensively used to probe energy transport properties in a number of branched and macromolecular architectures.[4] After obtaining parallel and perpendicular polarized fluorescence measurements, eq 1 was used to find the anisotropy.[47]

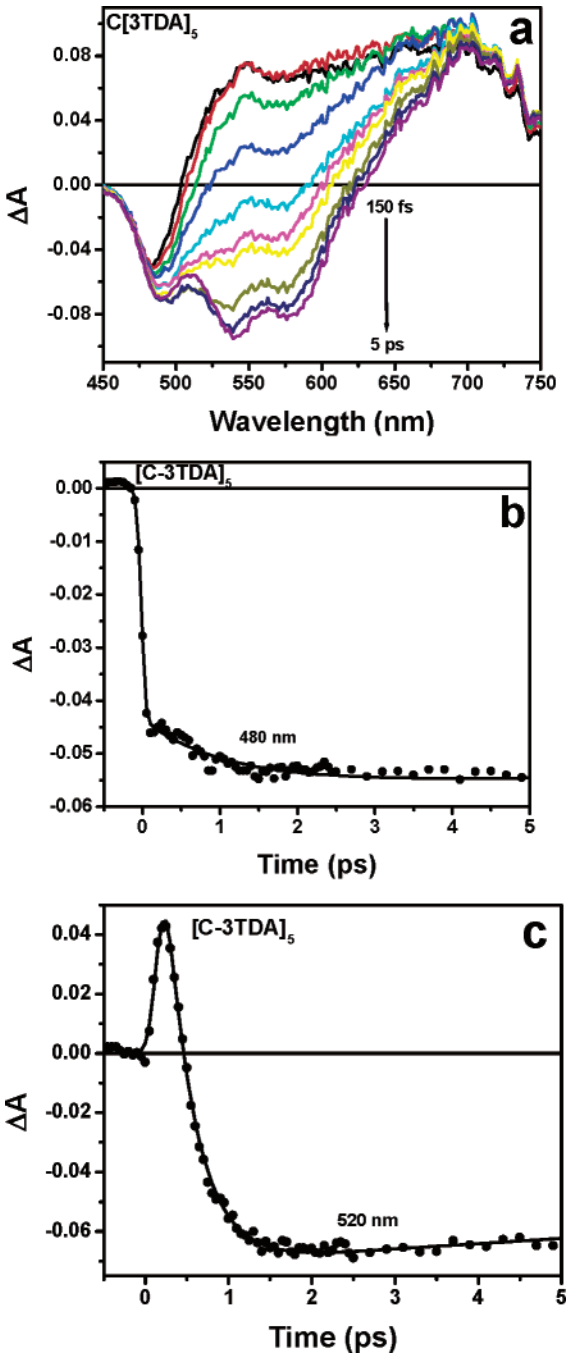

Figure 9. (a) Transient absorption spectra at of $[C\text{-}3TDA]_5$ in toluene in shorter time window from 150 fs to 5 ps after excitation at 420 nm. **(b)** Kinetic trace at 480 nm. (c) Kinetic decay trace at 520 nm.

$$\Gamma = \frac{I_{par} - I_{per}}{I_{par} + 2I_{per}} \quad (1)$$

Depolarization of the emission can be caused by a number of phenomena; for these molecules only two depolarization times were observed: one was very fast (less than 100 fs); the other was very slow (over 1 ns). The first depolarization is a fast process due to migration of the exciton to other chromophores

SCHEME 1: Energy Level Diagram for Cyclo(terthiophene-diacetylenes) C[3T-DA]$_2$ and C[3T-DA]$_5$[a]

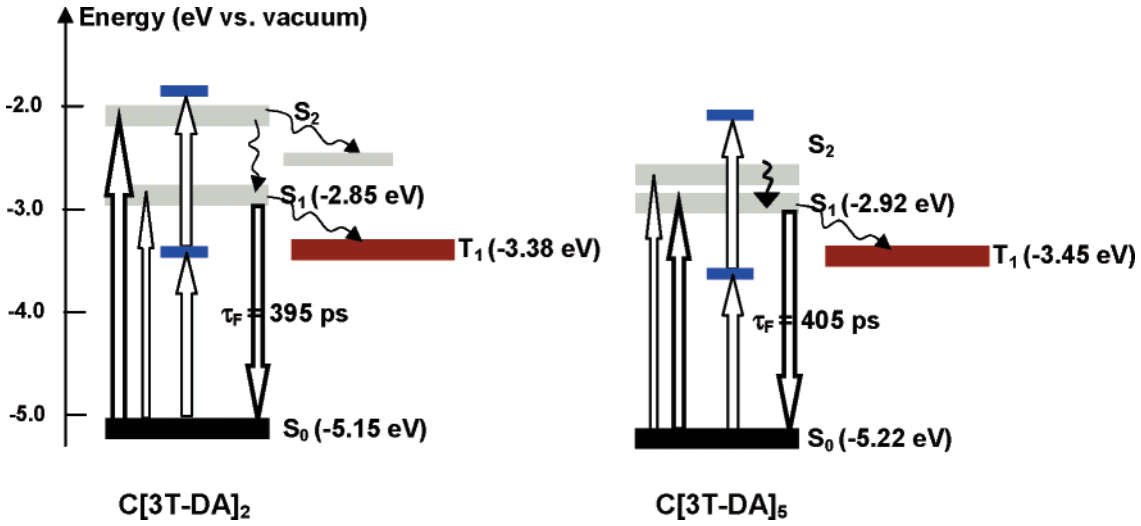

[a] The energies for the S_0 ground states are taken from cyclic voltammetry and the potential of the ferrocene/ferricenium reference electrode set to −4.8 eV vs vacuum. The other energy levels are taken from the optical investigation.

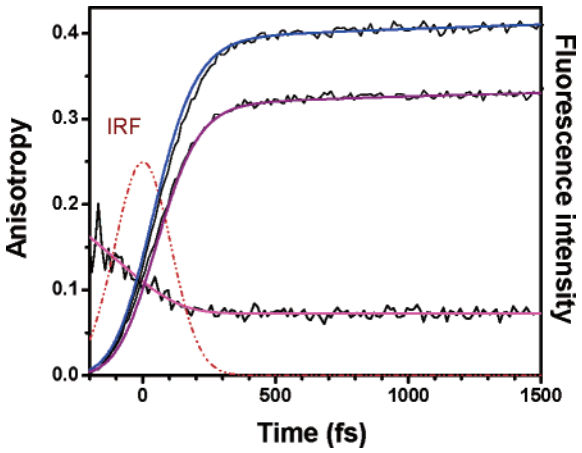

Figure 10. Raw data, shown in the parallel and perpendicular measurements above, convoluted with the instrument response function. A mathematical procedure removes the instrument response function leaving the experimental decay, shown in the anisotropy curve.

in the ring; the second depolarization is due to rotational diffusion. After deconvoluting the data from the instrument response function (Figure 10), it was found that the initial anisotropy decay in C[3T-DA]$_5$ was 27 ± 10 fs; this supports a coherent transport of excitons. A Förster hopping mechanism would be excluded with these results because Förster hopping occurs on the order of picoseconds. In this case, the Förster energy-transfer mechanism cannot be applied with physically reasonable parameters when energy transfer is so fast. Similarly, the system C[3T-DA]$_2$ has an initial anisotropy decay of 20 ± 10 fs; thus, our data support a coherent energy transport in both systems. We can compare these systems to the natural photosystem LH2 of the purple bacteria *Rhodobacter sphaeroides*, which has nine chromophores and experiences a combination of Förster and wavelike energy migration. The natural system LH2 presents two anisotropy decay times of 100 and 300−500 fs. The 100 fs time is too fast for Förster type energy migration, but the presence of the 300−500 fs decay supports the theory of an LH2 photosystem where the energy is delocalized over four chromophores and hops to the remaining chromophores.[48]

Initially, chromophore transition moments are oriented randomly in a plane, and the residual fluorescence anisotropy value is 0.4.[47] After the initial anisotropy decay, the steady-state anisotropy value of C[3T-DA]$_5$ was calculated to be 0.081 ± 0.01 with little observed anisotropy decay for up to 200 ps. The rotational diffusion time of C[3T-DA]$_5$ was crudely calculated using the Debye−Stokes−Einstein (DSE) equation to be longer than 1 ns, a time scale considerably longer than the time scales we observed, which explains why a significant drop in anisotropy up to 200 ps due to rotational diffusion was not observed.[47] The smaller ring system C[3T-DA]$_2$ had a anisotropy residual value of 0.11 ± 0.01, a decrease in anisotropy due to rotational diffusion was apparent, and by fitting the data to a exponential decay the rotational diffusion was calculated to be 850 ps. Terthiophene, an oligomer with three thiophene rings, has a rotational diffusion time of 175 ps.

We suggest that there are two ways for which we can account for the residual anisotropy of C[3T-DA]$_5$ being 0.081 ± 0.01 while the theoretical anisotropy for a planar system is 0.1. Either some fraction of the rings are deformed from a planar arrangement or the chromophores are twisted with respect to the plane of the molecule. Demidov and Andrews discussed the effect of chormophore orientation with respect to the plane of the ring on the residual anisotropy and obtained the following formula.[48]

$$R = 0.1(9\cos^4(\theta) - 6\cos^2(\theta) + 1) \qquad (2)$$

Using this formula, we can calculate that if the anisotropy of our system is 0.081 and a planar system is expected to have anisotropy of 0.1, then the difference could be explained if the chromophores' average inclination angle with respect to perpendicular is 7.9 ± 1°.

The average value for the anisotropy decay time was found to be 27 fs. Combining this with spectroscopic information can give us an idea of the type of energy transfer (exciton or hopping dynamics).[4,5] A large homogeneous line width would indicate strong interaction between the environment and the chromophores, lending to a hopping type energy transfer, while fast anisotropy decay times would indicate strong interaction between chromophores and lend to wavelike energy transfer.[4,5,49,50] This is a relatively simple approach which neglects inhomogeneous line broadening and can be quantified by an equation developed by Leegwater.[50] Equation 3 is a general expression for the anisotropy decay rate k_{dep} in a cyclic

system at high temperature.

$$k_{dep} = \Gamma\left(1 - \frac{1}{N}\sum_{k=1}^{N}\frac{\Gamma^2}{\Gamma^2 + 16J^2\sin^2\left(\frac{2\pi}{N}\right)\sin^2\left(\frac{2\pi k}{N}\right)}\right) \quad (3)$$

In this equation Γ is the homogeneous line width and N the number of chromophores. For a system of five chromophores the expression becomes eq 4.

$$k_{dep} = \frac{7.236\Gamma(\Gamma^2 + 7.236J^2)J^2}{(\Gamma^2 + 5J^2)(\Gamma^2 + 13.09J^2)} \quad (4)$$

We obtained plots of the decay time vs interaction strength to estimate the mode of energy transport in the thiophene macrocycles. Each curve represented a different value of Γ in eq 4. Utilizing this model, our time-resolved depolarization data places the anisotropy decay time at 27 fs, which according to Leegwater's theory would mean that excitation transfer in this system cannot be accounted for by pure Förster hopping mechanism and the excitation delocalization over a substantial part of the ring should be considered.

4. Conclusions

In conclusion, we have investigated the linear and nonlinear optical properties of two new conjugated macrocycles containing terthiophene-diacetylenes as repeat units. We were also able to experimentally examine the nature and coupling between the electronic states in these thiophene rings. The absorption spectrum for C[3T-DA]$_2$ showed almost decoupled S_1 and S_2 states, whereas C[3T-DA]$_5$ did not show because of the red shift of the S_2 state to close proximity of S_1 and possible stronger coupling between S_1 and S_2. Quantum yields at different excitations suggested the presence of an efficient nonradiative pathway from S_2 in the case of C[3T-DA]$_2$. Fluorescence emission and excitation spectra suggested the possibility of similar absorbing and emitting states for C[3T-DA]$_5$, while the absorption and emission states were found to be different for C[3T-DA]$_2$. TPA cross-section spectra determination showed that C[3T-DA]$_5$ showed a 550% enhancement over C[3T-DA]$_2$. Ultrafast transient absorption measurements elucidated the excited-state dynamics and provided the proof for the presence of S_1 and S_2 excited states in the case of C[3T-DA]$_2$ and C[3T-DA]$_5$. The presence of a triplet state is observed for both cyclothiophenes, and the ISC of S_1 to T_1 state provides an efficient nonradiative pathway. Fluorescence up-conversion measurements showed stronger inter-chromophore coupling within the macrocycles, and the excitation is delocalized on the major fraction of the ring. It has also shown a planarized geometry of the emitting state. We believe that the TPA cross-sections obtained for these thiophene rings are quite large and can be further enhanced by adding donor and acceptor groups to the cyclic systems, rendering them attractive for potential optical and possibly electronic applications.

Acknowledgment. T.G. acknowledges the Army Research Office and the National Science Foundation for support. The work at Ulm University has been supported by the German Research Foundation (DFG) in the frame of SFB 569.

References and Notes

(1) McQuade, D. T.; Hegedus, A. H.; Swager, T. M. *J. Am. Chem. Soc.* **2000**, *122*, 12389−12390.
(2) Franco, C.; Wilson, J. S.; Jasper, M. J.; Clement, D.; Silva, C.; Friend, R. H.; Severin, N.; Samori, P.; Rabe, J. P.; O'Connell, M. J.; Taylor, P. N.; Anderson, H. L. *Nat. Mater.* **2002**, *1*, 160.
(3) Bhaskar, A.; Ramakrishna, G.; Haley, M. M.; Goodson, T., III. *J. Am. Chem. Soc.* **2006**, *128*, 13972.
(4) (a) Goodson, T., III. *Acc. Chem. Res.* **2005**, *38*, 99. (b) Goodson, T., III. *Annu. Rev. Phys. Chem.* **2005**, 56, 581
(5) Varnavski, O. P.; Ostrowski, J. C.; Sukhomlinova, L.; Twieg, R. J.; Bazan, G. C.; Goodson, T., III. *J. Am. Chem. Soc.* **2002**, *124*, 1736.
(6) Wang, Y.; He, G. S.; Prasad, P. N.; Goodson, T., III. *J. Am. Chem. Soc.* **2005**, *127*, 10128.
(7) Albota, M.; et al. *Science* **1998**, *281*, 1653.
(8) Reinhardt, B. A.; Brott, L. L.; Clarson, S. J.; Dillard, A. G.; Bhatt, J. C.; Kannan, R.; Yuan, L.; He, G. S.; Prasad, P. N. *Chem. Mater.* **1998**, *10*, 1863.
(9) Mongin, O.; Porres, L.; Moreaux, L.; Mertz, J.; Blanchard-Desce, M. *Org. Lett.* **2002**, *4*, 719.
(10) Brunel, J.; Mongin, O.; Jutand, A.; Ledoux, I.; Zyss, J.; Blanchard-Desce, M. *Chem. Mater.* **2003**, *15*, 4139.
(11) Beljonne, D.; Wenseleers, W.; Zojer, E.; Shuai, Z.; Vogel, H.; Pond, S. J. K.; Perry, J. W.; Marder, S. R.; Bredas, J.-L. *Adv. Funct. Mater.* **2002**, *12*, 631.
(12) Wang, Y.; Ranasinghe, M. I.; Goodson, T., III. *J. Am. Chem. Soc.* **2003**, *125*, 9562.
(13) Varnavski, O. P.; Ostrowski, J. C.; Sukhomlinova, L.; Twieg, R. J.; Bazan, G. C.; Goodson, T., III. *J. Am. Chem. Soc.* **2002**, *124*, 1736.
(14) Katan, C.; Terenziani, F.; Mongin, O.; Werts, M. H. V.; Porre's, L.; Pons, T.; Mertz, J.; Tretiak, S.; Blanchard-Desce, M. *J. Phys. Chem. A* **2005**, *109*, 3024.
(15) Martin, R. E.; Diederich, F. *Angew. Chem., Intl. Ed.* **1999**, *38*, 1350.
(16) Meier, H. *Angew. Chem.* **1992**, *104*, 1425.
(17) Kraft, A.; Grimsdale, A. C.; Holmes, B. C. *Angew. Chem.* **1998**, *110*, 416.
(18) Loutfy, R. O.; Hor, A. M.; Hsiao, C. K.; Baranyi, G.; Kazmaier, P. *Pure Appl. Chem.* **1988**, *60*, 1047.
(19) Feringa, L.; Jager, W. F.; de Lange, B. *Tetrahedron* **1993**, *49*, 8267.
(20) Marsella, M. J.; Yoon, K.; Tham, F. S. *Org. Lett.* **2001**, *3*, 2129.
(21) Dürr, H. *Angew. Chem.* **1989**, *101*, 427.
(22) Kraft, A.; Grimsdale, A. C.; Holmes, B. C. *Angew. Chem.* **1998**, *37*, 403.
(23) Thompson, J.; Blyth, R. I. R.; Mazzeo, M. *Appl. Phys. Lett.* **2001**, *79*, 560.
(24) Katz, H. E.; Laquindanum, J. G.; Lovinger, A. J. *Chem. Mater.* **1998**, *10*, 633.
(25) Horowitz, G. *Adv. Mater.* **1998**, *10*, 365.
(26) Noma, N.; Tsuzuki, T.; Shirota, Y. *Adv. Mater.* **1995**, *7*, 647.
(27) Noda, T.; Imae, I.; Noma, N.; Shirota, Y. *Adv. Mater.* **1997**, *9*, 239.
(28) Fichou, D.; Nunzi, J. M.; Charra, F.; Pfeffer, N. *Adv. Mater.* **1994**, *6*, 64.
(29) McCullough, R. D. *Adv. Mater.* **1998**, *10*, 93.
(30) (a) *Handbook of Oligo- and Polythiophenes*; Fichou, D., Ed.; Wiley-VCH: Weinheim, Germany, 1999. Bäuerle, P. In *Electronic Materials: The Oligomer Approach*; Müllen, K. Wegner, G., Eds.; Wiley-VCH: Weinheim, Germany, 1998; pp 105−197. (b) Lightowler, S.; Hird, M. *Chem. Mater.* **2005**, *17*, 5538.
(31) Zhao, M.-T.; Singh, B. P.; Prasad, P. N. *J. Chem. Phys.* **1988**, *89*, 5535.
(32) Marder, S. R.; Kippelen, B.; Jen, A. K.; Peyghambarian, N. *Nature* **1997**, *388*, 845.
(33) Bednarz, M.; Reineker, P.; Mena-Osteritz, E.; Baeuerle, P. *J. Lumin.* **2004**, *110*, 225.
(34) Marsella, M. J. *Acc. Chem. Res.* **2002**, *35*, 944.
(35) Brault, L.; Miginau, E.; Neguesque, A.; Battaglia, E.; Bagrel, D.; Kirsch, G. *Eur. J. Med. Chem.* **2005**, *40*, 757.
(36) Sarkar, A.; Haley, M. M. *Chem. Commun. (Cambridge)* **2000**, 1733.
(37) Yamada, T.; Azumi, R.; Hiroaki, S.; Hideki, A.; Abe, M.; Baeuerle, P.; Matsumoto, M. *Chem. Lett.* **2001**, *10*, 1022.
(38) Kroemer, J.; Carreras, I. R.; Fuhrmann, G.; Musch, C.; Wunderlin, M.; Debaerdemaker, T.; Mena-Osteritz, E.; Baeuerle, P. *Angew. Chem., Intl. Ed.* **2000**, *39*, 3481.
(39) Chung, S.-J.; Kim, K.-S.; Lin, T.-C.; He, G. S.; Swiatkiewicz, J.; Prasad, P. N. *J. Phys. Chem. B* **1999**, *103*, 10741.
(40) Drobizhev, M.; Rebane, A.; Suo, Z.; Spangler, C. W. *J. Lumin.* **2005**, *111*, 291.
(41) Baeuerle, P. *Adv. Mater.* **1992**, *4*, 102.
(42) Fuhrmann, G.; Debaerdemaker, T.; Baurerle, P. *Chem. Commun. (Cambridge)* **2003**, 949.
(43) Maciejewski, A.; Steer, R. P. *J. Photochem.* **1986**, *35*, 59.
(44) Xu, C.; Webb, W. W. *J. Opt. Soc. Am. B* **1996**, *13*, 481.

(45) Beljonne, D.; Wenseleers, W.; Zojer, E.; Shuai, Z.; Vogel, H.; Pond, S. J. K.; Perry, J. W.; Marder, S. R.; Bredas, J.-L. *Adv. Funct. Mater.* **2002**, *12*, 631.
(46) Zhao, M.-T.; Singh, B. P.; Prasad, P. N. *J. Chem. Phys.* **1988**, *89*, 5535.
(47) Lakowicz, J. R. *Principles of Fluorescence Spectroscopy*; Kluwer Academic/Plenum: New York, 1999.
(48) Demidov, A.; Andrews, D. *Photochem. Photobiol.* **1996**, *63*, 39.
(49) Bradforth, S. E.; Jimenez, R.; van Mourik, F.; van Grondelle, R.; Fleming, G. *J. Phys. Chem.* **1995**, *99*, 16179.
(50) Leegwater, J. A. *J. Phys. Chem.* **1996**, *100*, 14402.
(51) Kumble, R.; Palese, S.; Visschers, R.; Dutton, P.; Hochstrasser, R. *Chem. Phys. Lett.* **1996**, *261*, 396.